

A Cryogenic Heat Transport System for Space-Borne Gimbaled Instruments

M.V. Zagarola¹, J.K. Sanders¹, and C.S. Kirkconnell²

¹Creare Inc., Hanover, NH

²Raytheon Space & Airborne Systems, El Segundo, CA

ABSTRACT

A key technical challenge facing future space-based target acquisition and tracking systems is the cooling of detectors and associated components mounted on a gimbal. A critical trade must be performed at the spacecraft-level to determine whether to place the cryocooler on or off the gimbal. The off-gimbal approach has the advantage of removing the mass of the cryocooler and ambient-temperature heat rejection system from the gimbal, but requires a cryogenic heat transport system to exchange heat from on-gimbal components to the cryocooler. Creare and Raytheon are currently developing a heat transport system that uses a single-phase gaseous flow loop. The flow loop consists of ultra-flexible tubing to impart minimal torque to the gimbal motors, a miniature cryogenic circulator to pump the cycle gas with minimal input power, and thermally effective heat exchangers to transport heat with high conductance. The heat transport system has heritage in the NICMOS heat transport system developed by Creare and operational since 2002 on the Hubble Space Telescope. This paper describes the design of the cross-gimbal system, the test results from cryogenic life and flexibility tests on the flexible tubing, and our progress towards a demonstration of a two-stage cryogenic heat transport system.

INTRODUCTION

Future space-based target acquisition and tracking systems will require reliable and efficient cooling systems for gimbal-mounted infrared sensors and optics. A candidate cooling approach uses a high-performance, off-gimbal cryocooler with a high-conductance, cryogenic heat transport system to exchange heat from the sensors to the cryocooler. To meet typical mission requirements, the heat transport system must have high reliability, low mass, and high conductance; impart minimal torque to the gimbal; and produce minimal parasitic heat loads to the cryocooler. To meet these challenging requirements, Creare and Raytheon are developing a cryogenic heat transport system that uses a miniature, high-performance circulator to pump a single-phase gas through a loop consisting of ultra-flexible transfer lines and high-performance heat exchangers.

Schematics of the cycle are shown in Figure 1. A miniature cryogenic circulator located on a stationary platform circulates fluid between an on-gimbal load heat exchanger and an off-gimbal cryocooler interface heat exchanger. The fluid flows between the platform and the gimbal through miniature flexible transfer lines that are sized to create an acceptable fluid resistance and impose minimal torque on the gimbal. The overall heat transport system is compact and lightweight, produces no vibration on the gimbal, simplifies the cross-gimbal thermal and electrical interfaces, and

increases overall system reliability. As shown in Figure 1, the heat transport system can be configured for single-stage or multistage heat transport through the addition of one or more recuperators. The use of recuperators permits a single circulator to be placed at the higher temperature stage, which reduces cryocooler input power.

This paper describes the key components of the heat transport system, the packaging and integration of the heat transport system with a prototypical gimbal, the results of cryogenic life and flexibility tests on the transfer lines, and our progress towards demonstration of a two-stage cryogenic heat transport system.

HEAT TRANSPORT LOOP DESIGN

Performance targets representative of missile tracking application were used to design the heat transport system (see Table 1). The system components were designed to meet or exceed these targets. The key uncertainty in the system design was associated with the life and flexibility of the transfer lines. Consequently, cryogenic life and flexibility tests were performed on these components at the start of this program. The results of these tests are described later in this paper.

A concept for integrating a two-stage heat transport system with a gimbal is shown in Figure 2. The transfer lines are configured for a rotary motion of $\pm 200^\circ$ about the azimuth axis and $\pm 90^\circ$

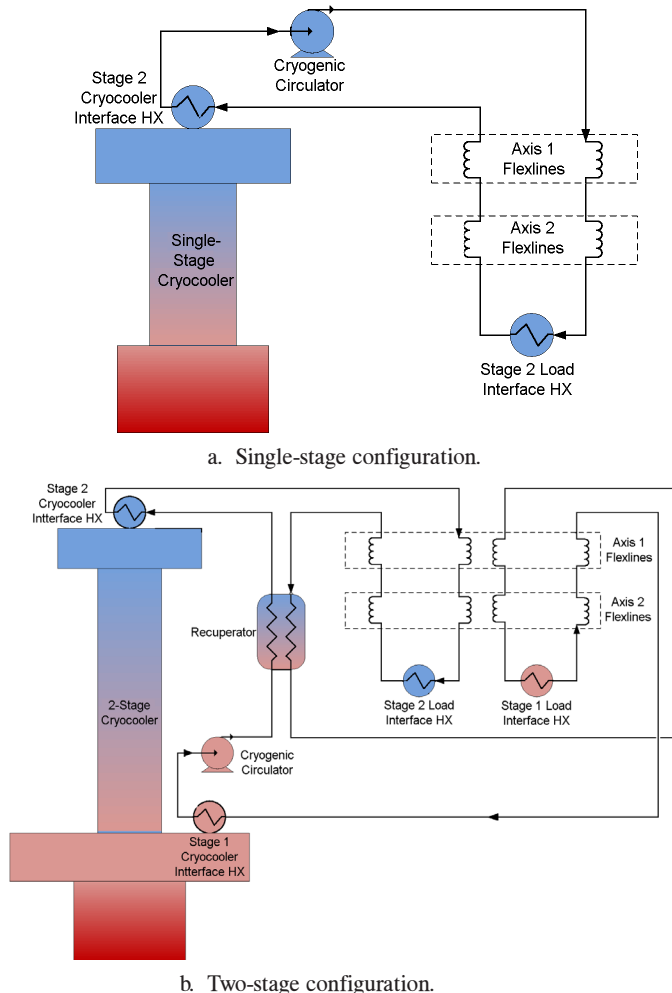


Figure 1. Cryogenic circulating loop for cross-gimbal cooling.

Table 1. Performance targets for cryogenic heat transport system.

Rotation	$\pm 200^\circ$ 1st axis, $\pm 90^\circ$ 2nd axis
Maximum Angular Velocity	$200^\circ/\text{s}$
Maximum Angular Acceleration	$200^\circ/\text{s}^2$
Torque Imparted to Gimbal	$< 70 \text{ mN}\cdot\text{m}$ (10 oz-in.)
Cold Load Temperature	35 K
Average Cold Load	2 W

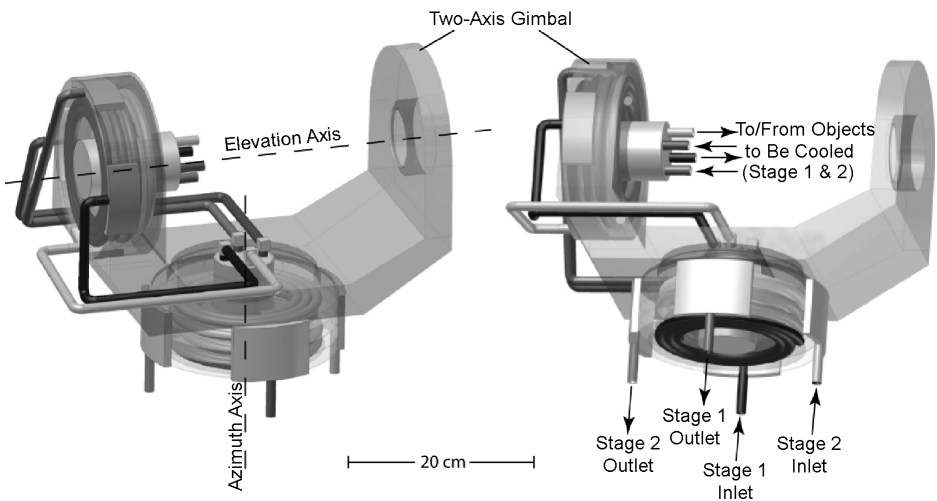


Figure 2. Gimbal integration concept.

about the elevation axis. The inflow and outflow transfer lines are configured as counter-rotating coils about each axis and are packaged within a casing that is actively cooled by the Stage 1 cryocooler. The on-gimbal components that impart inertia to the gimbal motors consist of load interface heat exchangers for both cooling stages, the flexline casing for the elevation axis, the flexlines and rigid tubes. The system is designed to transport 2 W of heat at 35 K and to intercept parasitics at a Stage 1 temperature of 85-100 K. The overall heat transport system mass is approximately 9 kg, and only 3 kg of the total mass is supported on the gimbal. The on-gimbal mass for this heat transport system is significantly less than an approach that locates the cryocooler and heat rejection system on-gimbal and leads to significant reductions in payload mass due to smaller gimbal motors and counterbalances.

The circulator operating speed and system operating pressure were determined by trading conductance of the loop with parasitics associated with the heat transport system. The increase in flexline stiffness due to internal pressure and the maximum allowable pressure of the system components were also considered, but did not influence the final design and operating conditions. The operating conditions were selected to minimize the total input power, which includes cryocooler and circulator input power. The optimum temperature difference between the Stage 2 cold head of the cryocooler and the sensor interface is 5 K. The parasitics due to the heat transport loop (recuperator loss plus radiative parasitics) absorbed by the Stage 2 cryocooler are 0.5 W. An additional 1.5 W of heat is absorbed by the Stage 1 cryocooler at 85 K and is used to cool the flexline casing to about 100 K for shielding the flexlines from the ambient temperature environment. The conductance of the loop is 0.4 W/K. The heat transport system is scalable to loads from 1 W to 20 W and temperatures from about 20 K to 140 K through optimization of the operating conditions.

The key components for the heat transport system are the circulator, flexible transfer lines, and interface heat exchangers and are applicable to single- and multistage configurations. The circulator is identical to the circulator used in NASA's NICMOS Cooling System program, which has

operated for over six years in space without any change in performance¹ and is shown in Figure 3 during cryogenic qualification testing. This circulator has demonstrated high efficiency, low input power, and high reliability. It has been tested at input power levels as low as 50 mW, temperatures down to approximately 70 K, and with multiple cycle gases including neon and helium. The basic turbomachine design is identical to the cryogenic turboalternators manufactured by Creare, which have been tested at power levels up to 30 W and temperatures down to 12 K. The flexible transfer lines are manufactured using miniature bellows similar to those shown in Figure 4. They are sized for this application to produce acceptable pressure drop and to impart minimal torque on the gimbal. The flexlines also can be used to effectively isolate the gimbal-mounted optics and sensors from deleterious vibration on the spacecraft, which is important for some applications.

The flight design of the interface heat exchangers is shown in Figure 5. The same design can be used for the load and cryocooler interface heat exchangers. The cycle gas flows axially into the heat exchanger and then radially outward through the fins. For the load/cryocooler interface heat exchanger, heat is conducted from/to the base of the heat exchanger to/from the fins where it is convected to/from the cycle gas. The key features of these heat exchangers are good thermal performance (effectiveness of greater than 0.95), low pressure drop, compactness, low mass (0.1 kg), and good temperature uniformity at the mounting surface. The heat exchanger design is based on the NICMOS aftercooler. The miniature slots between fins are made using an electric discharge machining process for high precision at small scales. The fin material is copper for high conductivity and excellent thermal performance.

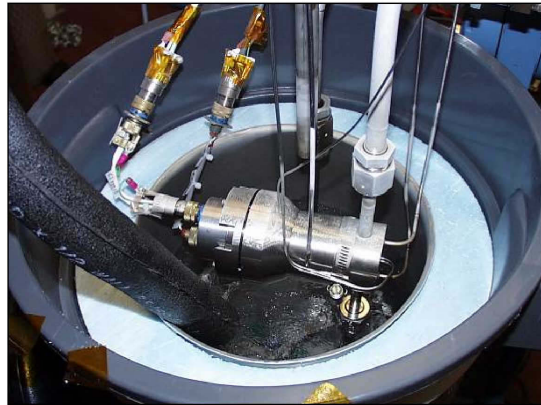


Figure 3. NICMOS circulator submerged in liquid nitrogen during cryogenic qualification tests.

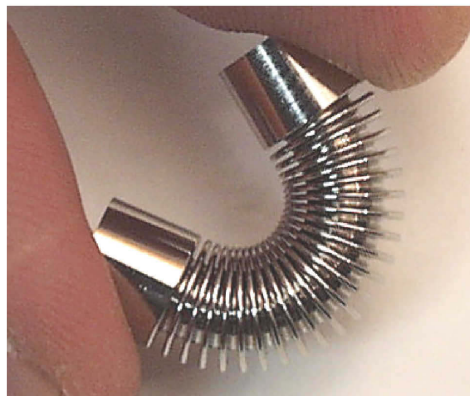


Figure 4. Miniature flexible bellows used in flexlines.

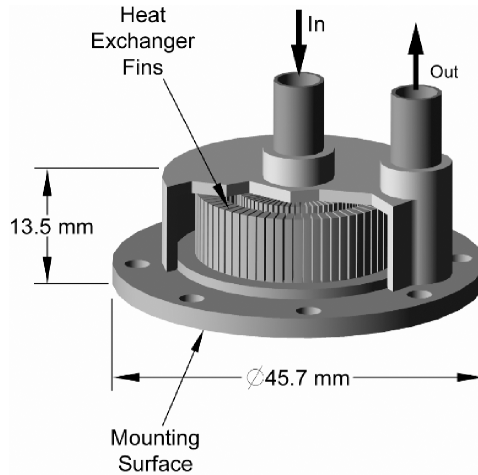


Figure 5. Interface heat exchanger schematic.

The remaining components consist of a recuperator to transfer heat from the inflow to outflow stream, rigid tubes to connect components, an accumulator to maintain acceptable internal pressures when the system is warm, and drive electronics to provide power and speed control for the circulator. These remaining components have modest performance requirements and straightforward designs.

CRYOGENIC FLEXLINE TESTING

A cryogenic test facility was constructed and used to quantify the relationship between torque and angle of rotation on a prototypical flexline at ambient and cryogenic temperatures. The facility is shown in Figure 6. The facility permitted testing the flexlines over a range of motion of $\pm 200^\circ$ in one axis. During cryogenic tests, liquid nitrogen is used to maintain the flexlines at approximately 80 K. An in-line torque meter, connected to the bellows through an actuation arm, is used to measure the torque required to rotate the flexlines. The flexlines are installed in a casing, which is shown in Figure 7. The casing includes shelves coated with Teflon to reduce friction during testing in 1-g.

FLEXIBILITY TEST RESULTS

Tests were performed in 1-g at room temperature and 80 K. The results of the torque test are summarized in Table 2. A single flexline was tested in a spiral configuration as shown in Figure 7. The flexline was tested at 300 K and 80 K and at an internal pressure of 7.7 atm. (100 psig) to provide a conservative upper limit of the pressure difference across the bellows during normal operation in a vacuum (~ 3 atm. for the 35 K system). The angle of rotation was $\pm 200^\circ$ at 300 K and $\pm 180^\circ$ at 80 K. The reduced rotation at cryogenic temperatures avoided over-stroking the flexlines and was required because the bellows length was initially optimized for operation at 300 K. The range of maximum angular velocity and acceleration was 50-400°/s and 50-400°/s², respectively.

The torque measurements at cryogenic temperatures, over several actuations and after nominally 41,000 and 500,000 cycles, are shown in Figure 8. Due to the low torque values, the measurements show some noise that was determined to be associated with the stepper motor. A line through the data is shown in Figure 8 representing a moving average of the data. The peak torque was approximately 80 mN-m at 80 K. In a prototypical configuration, the inlet and outlet flexlines are arranged to form counter-rotating spirals about each axis of rotation. Therefore, when one spiral is winding, the other spiral is unwinding, which will reduce the peak torque of a flexline pair to a value below those reported for a single flexline.

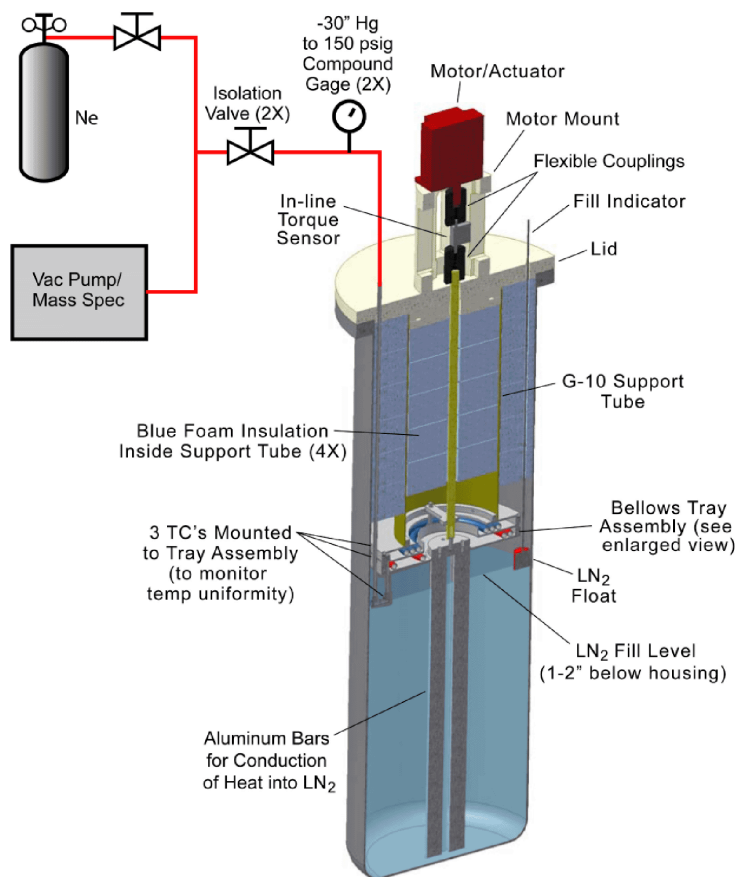


Figure 6. Schematic of cryogenic flexline test facility.

Table 2. Torque test summary.

Test Setup		
Temperature	300 K	80 K
Number of Coils	Single	Single
Internal Pressure	7.7 atm (100 psig)	7.7 atm (100 psig)
Fill Gas	Ne	Ne
Rotation	±200°	±180°
Results		
Actuation Profile	Max/Min Torque Values (mN-m)	
50°/s, 50°/s ²	+70/-20	+85/-35
50°/s, 100°/s ²	+70/-25	+84/-29
50°/s, 200°/s ²	+70/-23	+81/-28
50°/s, 400°/s ²	+71/-25	+80/-28
100°/s, 100°/s ²	+71/-22	+85/-25
100°/s, 200°/s ²	+70/-22	+83/-25
100°/s, 400°/s ²	-	+82/-23
200°/s, 200°/s ²	-	+83/-21
200°/s, 400°/s ²	+71/-24	+82/-20
400°/s, 400°/s ²	+70/-22	+82/-20

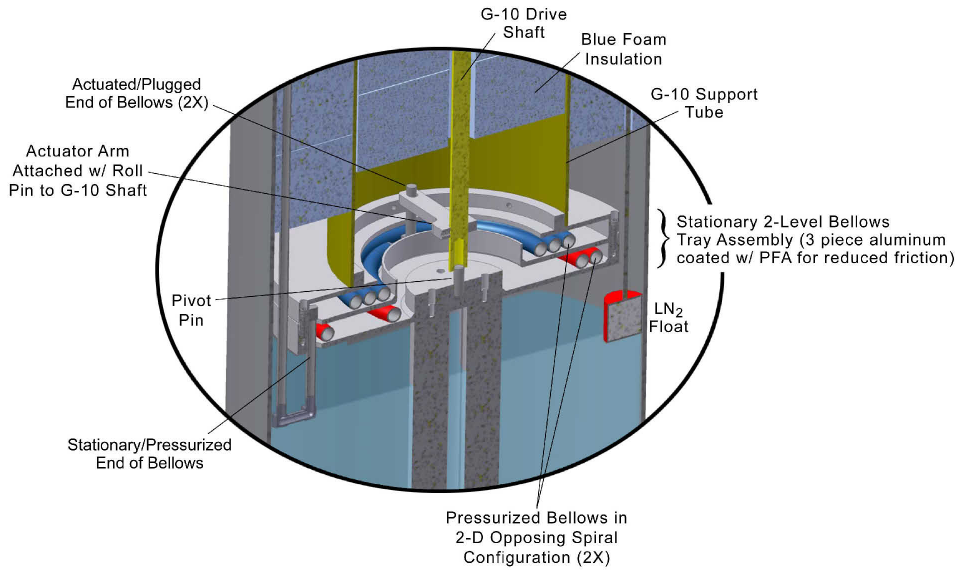


Figure 7. Schematic of flexlines installed in casing in test facility.

LIFE TEST RESULTS

The lifetime of the flexlines was investigated by executing over 500,000 full actuation cycles at cryogenic temperatures and prototypical pressure. The actuation profile was $\pm 180^\circ$ and at a peak velocity and acceleration of $200^\circ/\text{s}$ and $200^\circ/\text{s}^2$, respectively. The flexlines were identical to those used in the flexibility tests. The tests required five weeks of continuous operation to complete. The metric to identify a failure during testing was a change in torque or a change in internal pressure. In addition, after the life test, a helium leak test and visual inspection were performed to identify failures and wear.

The measured torque after 500,000 cycles is also shown in Figure 8. Only a minimal change in the torque profile was observed, which was attributed to a small amount of wear in the actuator, test hardware, and flexlines. In addition, no change in the internal pressure was observed during testing. At the completion of 500,000 cycles, we performed a helium leak test on the flexlines that verified that the flexlines were still hermetic with a helium leak rate of less than 10^{-9} std cc/sec.

SUMMARY AND FUTURE PLANS

A two-stage cryogenic heat transport system was designed that will significantly reduce mass of gimbal-mounted payloads. The heat transport system has been optimized to transport 2 W at 35 K with additional heat transport at 85-100 K. It has high reliability, low mass, and high conductance; imparts minimal torque to the gimbal; emits no vibration; and produces minimal parasitic heat loads to the cryocooler. The system consists of a miniature cryogenic circulator that has space heritage, high-performance heat exchangers, and flexible transfer lines. The overall heat transport system mass is approximately 9 kg, with only 3 kg of the total heat transport system mass supported on the gimbal. The on-gimbal mass for this heat transport system is significantly less than an approach that locates the cryocooler and heat rejection system on-gimbal. The heat transport system is scalable to loads from 1 W to 20 W and temperatures from about 20 K to 140 K through optimization of the operating conditions.

The key technical risks of the technology were the flexibility and lifetime of the transfer lines. The flexibility of the transfer lines was demonstrated by test in a prototypical configuration and operating conditions. The lifetime of the transfer lines was demonstrated by completing over

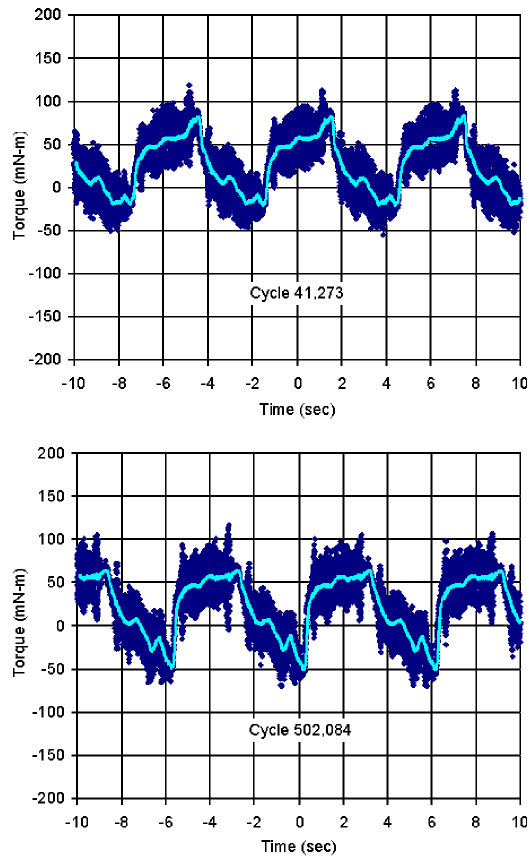


Figure 8. Torque measurements at 41,000 and 500,000 cycles.

500,000 actuation cycles at a temperature of 80 K, at a pressure in excess of the nominal operating pressure, and at the maximum angular acceleration and velocity expected for a gimbal system.

Creare and Raytheon are currently developing a ground demonstration unit to be tested in a thermal vacuum chamber. The system will include the complete two-stage heat transport system interfaced with a two-stage cryocooler and packaged into a test gimbal. A resistive heater will be used to simulate a sensor load on the gimbal. The test program has been structured to obtain the following quantities of interest: heat transport capacity, conductance, parasitics, lifetime, mass, and torque imparted on the gimbal. The thermal vacuum tests are scheduled for the spring of 2009.

ACKNOWLEDGMENTS

The support and guidance provided by the Missile Defense Agency and the Air Force Research Laboratory are gratefully acknowledged.

REFERENCES

1. Swift, W.L., Dolan, F.X., and Zagarola, M.V., "The NICMOS Cooling System – 5 Years of Successful On-Orbit Operation," *Adv. in Cryogenic Engineering*, Vol. 53, Amer. Institute of Physics, Melville, NY (2008), pp. 799-806.